

Solid-State Chelation of Metal Ions by Ethylenediaminetetraacetate Intercalated in a Layered Double Hydroxide

Konstantin A. Tarasov and Dermot O'Hare*

Inorganic Chemistry Laboratory, South Parks Road, Oxford OX1 3QR, U.K.

Vitaly P. Isupov

Institute of Solid State Chemistry and Mechanochemistry, Siberian Branch of Russian Academy of Science, Kutateladze 18, Novosibirsk 630128, Russia

Received June 10, 2002

The solid-state chelation of transition metal ions (Co^{2+} , Ni^{2+} , and Cu^{2+}) from aqueous solutions into the lithium aluminum layered double hydroxide ($[\text{LiAl}_2(\text{OH})_6]\text{Cl}\cdot 0.5\text{H}_2\text{O}$ or LDH) which has been pre-intercalated with EDTA (ethylenediaminetetraacetate) ligand has been investigated. The intercalated metal cations form $[\text{M}(\text{edta})]^{2-}$ complexes between the LDH layers as indicated by elemental analysis, powder X-ray diffraction, and IR and UV–vis spectroscopies. If metal chloride or nitrate salts are used in the reaction with the LDH then co-intercalation of either the Cl^- or NO_3^- anions is observed. In the case of metal acetate salts the cations intercalate without the accompanying anion. This can be explained by the different intercalation selectivity of the anions in relation to the LDH. In the latter case the introduction of the positive charge into LDH structure was compensated for by the release from the solid of the equivalent quantity of lithium and hydrogen cations. Time-resolved in-situ X-ray diffraction measurements have revealed that the chelation/intercalation reactions proceed very quickly. The rate of the reaction found for nickel acetate depends on concentration as $\sim k[\text{Ni}(\text{Ac})_2]^3$.

Introduction

Layered double hydroxides (LDHs) being typical intercalation compounds are of considerable interest due to their valuable and unique ion-exchange intercalation properties. Their general formula can be presented as $[\text{M}^{2+}_{1-x}\text{M}^{3+}_x(\text{OH})_2]^{x+}(\text{A}^{n-})_{x/n}\cdot m\text{H}_2\text{O}$, where $\text{M}^{2+} = \text{Mg}^{2+}$, Ni^{2+} , Co^{2+} , Zn^{2+} , Ca^{2+} , etc. and $\text{M}^{3+} = \text{Al}^{3+}$, Cr^{3+} , Fe^{3+} , Mn^{3+} , etc. The only exception among LDHs is when $\text{M}^{2+} = \text{Li}^+$ giving rise to $\{[\text{LiAl}_2(\text{OH})_6]^+\}_n\text{A}^{n-}\cdot m\text{H}_2\text{O}$ (Li,Al-LDH-A). Its structure consists of positively charged layers $[\text{LiAl}_2(\text{OH})_6]^+$ separated by interlayer anions A^{n-} and solvent molecules.

In recent years great attention has been given to LDHs, which contain interlayer organic chelating ligands: EDTA (ethylenediaminetetraacetate), NTA (nitrotriacetate), and their complexes with metals.^{1–9} It has been shown that such intercalates are convenient precursors for the preparation of composite materials containing metal nanoparticles^{10,11} or

semiconductors^{12,13} and can be used for the preparation of ternary metal oxides.^{9,14,15}

(1) Sissoko, I.; Iyagba, E. T.; Sahai, R.; Biloen, P. J. *Solid State Chem.* **1985**, *60*, 283–8.
(2) Narita, E.; Yamagishi, T.; Tazawa, K.; Ichijo, O.; Umetsu, Y. *Clay Sci.* **1995**, *9*, 187.

(3) Isupov, V. P.; Tarasov, K. A.; Chupakhina, L. E.; Mitrofanova, R. P.; Skvortsova, L. I.; Boldyrev, V. V.; Russ, J. *Inorg. Chem.* **1995**, *1*, 22.
(4) Isupov, V. P.; Tarasov, K. A.; Chupakhina, L. E.; Mitrofanova, R. P.; Boldyrev, V. V. *Dokl. Chem.* **1994**, *1–3*, 90.
(5) Kaneyoshi, M.; Jones, W. J. *Mater. Chem.* **1999**, *9*, 805.
(6) Gutmann, N. H.; Spiccia, L.; Turney, T. W. *J. Mater. Chem.* **2000**, *5*, 1219.
(7) Isupov, V. P.; Chupakhina, L. E.; Tarasov, K. A.; Boldyrev, V. V. *Dokl. Chem.* **1996**, *1–3*, 126.
(8) Tsyganok, A. I.; Suzuki, K.; Hamakawa, S.; Takehira, K.; Hayakawa, T. *Chem. Lett.* **2001**, *1*, 24.
(9) Kaneyoshi, M.; Jones, W. *Mol. Cryst. Liq. Cryst.* **2001**, *356*, 459.
(10) Isupov, V. P.; Tarasov, K. A.; Mitrofanova, R. P.; Chupakhina, L. E. In *Nanophase and Nanocomposites Materials II (MRS Proceedings)*; Komarneni, S., Parker, J. C., Wollenberger H. J., Eds.; Materials Research Society: New York, 1997; Vol. 457, p 539.
(11) Tarasov, K. A.; Isupov, V. P.; Bokhonov, B. B.; Gaponov, Yu. A.; Tolochko, B. P.; Sharafutdinov, M. R.; Shatskaya, S. S. *J. Mater. Synth. Proc.* **2000**, *1*, 21.
(12) Sato, T.; Okuyama, H.; Endo, T.; Shimada, M. *React. Solids* **1990**, *8*, 63.
(13) Sato T.; Masaki, K.; Yoshioka, T.; Okuwaki, A. *J. Chem. Technol. Biotechnol.* **1993**, *58*, 315
(14) Tarasov, K. A.; Isupov, V. P.; Chupakhina, L. E. *Russ. J. Inorg. Chem.* **2000**, *11*, 1659.

In this work, the formation of Co^{2+} , Ni^{2+} , and Cu^{2+} complexes of EDTA within the interlayer space of an LDH has been studied. It is well-known that the EDTA ligand forms very stable complexes in solution with almost any metal; for example, logarithms of stability constants for binding to Co^{2+} , Ni^{2+} , and Cu^{2+} are 16.3, 18.6, and 18.8, respectively.¹⁶ We were interested to see if we could prepare a solid-state version of EDTA by initially intercalating EDTA into an LDH and then using this resulting EDTA/LDH complex as a solid state complexation material for metal ions. This approach may be of interest as a method for recovering transition and/or radioactive metals from aqueous solutions.

We began by considering the possibility of anion-exchange intercalation of EDTA into an LDH to give $\text{LDH-H}_n\text{Y}$, (where $\text{H}_n\text{Y}^{(4-n)-}$ is one of the four possible anions of EDTA). At 20 °C EDTA exhibits the following aqueous dissociation constants: $\text{p}K_1 = 2.00$, $\text{p}K_2 = 2.66$, $\text{p}K_3 = 6.16$, and $\text{p}K_4 = 10.24$. In the interval pH 4–10 (the most appropriate for anion exchange in LDHs) the ligand exists predominantly as $[\text{H}_2\text{Y}]^{2-}$ and/or $[\text{HY}]^{3-}$ anions, and pH 4.5 and 8.0 are the corresponding pH values of their maximal equilibrium concentrations.^{17,18} According to the preliminary data obtained previously,⁴ treatment of Li,Al-LDH-Cl with EDTA solutions at the fixed pH values can lead to the replacement of chloride ions predominantly by either $[\text{H}_2\text{Y}]^{2-}$ or $[\text{HY}]^{3-}$. Similar results have been observed for Zn,Cr-LDH-NO_3 upon intercalation of nitriotriacetates Hnta^{2-} and nta^{3-} at pH ~ 6.7 and 11, respectively.⁶

The next step in the formation of $[\text{MY}]^{2-}$ complexes within an LDH structure is the treatment of the preformed $\text{LDH-H}_n\text{Y}$ intercalate with a solution of a metal salt. In water solution chelating rapidly occurs according to the following equation:



However, in solid state this reaction may be complicated by the necessity to intercalate not only M^{2+} cations, but accompanying anions as well. As seen from the equation above, only in case of H_2Y^{2-} and H_3Y^- this reaction proceeds as “cation exchange” of one M^{2+} for two H^+ . In the case where the ligand is less protonated ($n < 2$), complex formation would cause an excessive positive charge in the LDH, which is likely to be compensated for by intercalating additional anions that are present in the solution. Such a process was first supposed by the authors in ref 3 and was later shown to take place in Zn,Cr-LDH-nta .⁶ Treatment of Zn,Cr-LDH-nta with copper and nickel chlorides or nitrates

led to the insertion of the metal cations together with the additional charge-compensating anions (Cl^- or NO_3^-) into the LDH.

In the case of Li,Al-LDH another mechanism of the charge compensation may exist.³ This host is the only known LDH which can be prepared through the direct intercalation of both cations and anions into a crystalline hydroxide.^{19–21} This process has been shown to be reversible to such an extent that it is possible to completely deintercalate Li^+ and the charge compensating interlayer anions, giving high-purity $\text{Al}(\text{OH})_3$.²² For that reason, the charge compensation upon the complex formation within this LDH can also occur through the release of lithium cations from the structure.

The aim of this work was to investigate the chelation process between the ligand EDTA and the transition metals Co, Ni, and Cu taking place within the interlayer space of Li,Al-LDH .

Experimental Section

Synthesis of Li,Al-LDH-Cl , $\text{Li,Al-LDH-H}_2\text{Y}$, and Li,Al-LDH-HY . The layered double hydroxide Li,Al-LDH-Cl ($[\text{LiAl}_2(\text{OH})_6\text{Cl}\cdot 0.5\text{H}_2\text{O}]$) used in further anion-exchange reactions was prepared by treatment of gibbsite $[\gamma\text{-Al}(\text{OH})_3]$ with concentrated LiCl water solution as described in ref 20. $\text{Li,Al-LDH-H}_2\text{Y}$ was prepared by suspending 2 g of Li,Al-LDH-Cl in 100 mL of a 0.075 M aqueous solution of H_4Y . Li,Al-LDH-HY was prepared by suspending 5 g of Li,Al-LDH-Cl in 90 mL of a 0.13 M aqueous solution of $\text{Na}_2\text{H}_2\text{Y}$. In both cases NaOH was added beforehand to adjust the solutions to pH 4.5 and 8.0, respectively. The reaction mixture was kept at room temperature for 1 h with constant stirring; thereafter the solids were filtered, washed with deionized water, and dried at ~ 50 °C in air.

Anal. Found/calcd (%). For $[\text{LiAl}_2(\text{OH})_6\text{Cl}\cdot 0.5\text{H}_2\text{O}]$ (Li,Al-LDH-Cl): Al, 25.63/26.02; Li, 3.39/3.35; Cl, 17.56/17.09; H, 3.58/3.40. For $[\text{LiAl}_2(\text{OH})_6(\text{C}_{10}\text{H}_{14}\text{N}_2\text{O}_8)_{0.46}\text{Cl}_{0.08}\cdot 2.5\text{H}_2\text{O}]$ ($\text{Li,Al-LDH-H}_2\text{Y}$): Al, 15.81/15.67; Li, 1.93/2.02; Cl, 0.89/0.83; C, 15.75/16.05; H, 4.55/5.11; N, 3.48/3.74. For $[\text{LiAl}_2(\text{OH})_6(\text{C}_{10}\text{H}_{13}\text{N}_2\text{O}_8)_{0.33}\cdot 2.5\text{H}_2\text{O}]$ (Li,Al-LDH-HY): Al, 17.54/17.78; Li, 2.13/2.29; Cl, 0.10/0; C, 12.48/13.06; H, 4.93/5.08; N, 2.86/3.05.

Synthesis of Li,Al-LDH-MY and $\text{Na}_2[\text{MY}]\cdot x\text{H}_2\text{O}$. The intercalates Li,Al-LDH-MY ($[\text{LiAl}_2(\text{OH})_6(\text{MY})_{0.5}\cdot 3\text{H}_2\text{O}]$, $\text{M} = \text{Co}^{2+}$, Ni^{2+} , Cu^{2+}) were prepared by direct anion exchange by suspending 2 g of the Li,Al-LDH-Cl in 75 mL of a 0.2 M aqueous solution of $\text{Na}_2[\text{MY}]$ at 90 °C for 1 h with constant stirring. The final products were filtered, washed with deionized water, and dried at ~ 50 °C in air. The metal EDTA complexes ($\text{Na}_2[\text{MY}]\cdot x\text{H}_2\text{O}$) were prepared according to the procedure.²³ The $\text{Na}_2[\text{MY}]\cdot x\text{H}_2\text{O}$ complexes were prepared by taking the appropriate basic metal carbonate and adding it to a ~ 0.1 M solution of $\text{Na}_2\text{H}_2\text{Y}$ at 100 °C for 2 h; the solutions were filtered to separate the excessive solids. The salts were crystallized by evaporating the solutions to one-third the initial volume and cooling in ice; afterward diethyl ether was added to give rise to precipitation of $\text{Na}_2[\text{MY}]\cdot x\text{H}_2\text{O}$.

(15) Tsyganok, A. I.; Suzuki, K.; Hamakawa, S.; Takehira, K.; Hayakawa, T. *Catal. Lett.* **2001**, *1–3*, 75.

(16) Dyatlova, N. M.; Temkina, V. Ya.; Popov, K. I. *Kompleksny i kompleksonaty metallov (Complexones and Metal Complexonates)*; Khimiya: Moscow, **1988**; p 544.

(17) Anderegg, G. In *Comprehensive coordination chemistry*. Wilkinson, Ed.; Pergamon: New York, 1987; p 777.

(18) Martell, A. E.; Smith, R. M. *Critical stability constants*; Plenum Press: New York, London, 1974; Vol. 1. Martell, A. E.; Smith, R. M. *Critical stability constants*; Plenum Press: New York, London, 1982; Vol. 5.

(19) Nemudry, A. P.; Isupov, V. P.; Kotsupalo, N. P.; Boldyrev, V. V. *React. Solids* **1986**, *1*, 221.

(20) Besserguenev, A. V.; Fogg A. M.; Francis, R. J.; Price, S. J.; O'Hare, D.; Isupov, V. P.; Tolochko, B. P. *Chem. Mater.* **1997**, *9*, 241.

(21) Fogg, A. M.; O'Hare, D. *Chem. Mater.* **1999**, *11*, 1771.

(22) Isupov, V.; Chupakhina, L.; Belobaba, A.; Trunova, A. *J. Mater. Synth. Process.* **1999**, *1*, 9.

(23) Radko, V. A.; Yakimets, Ye. M. *Zh. Neorgan. Khim.* **1962**, *7*, 683.

Anal. Found/calcd (%). For $[\text{LiAl}_2(\text{OH})_6](\text{CoC}_{10}\text{H}_{12}\text{N}_2\text{O}_8)_{0.5} \cdot 3\text{H}_2\text{O}$ (Li,Al-LDH-CoY): Al, 14.03/13.82; Li, 1.79/1.78; Co, 7.48/7.54; Cl, 0.89/0; C, 15.23/15.38; H, 4.61/4.65; N, 3.41/3.59. For $[\text{LiAl}_2(\text{OH})_6](\text{NiC}_{10}\text{H}_{12}\text{N}_2\text{O}_8)_{0.5} \cdot 3\text{H}_2\text{O}$ (Li,Al-LDH-NiY): Al, 14.85/13.82; Li, 1.68/1.78; Ni, 7.02/7.52; Cl, 0.49/0; C, 14.83/15.38; H, 4.80/4.65; N, 3.30/3.59. For $[\text{LiAl}_2(\text{OH})_6](\text{CuC}_{10}\text{H}_{12}\text{N}_2\text{O}_8)_{0.5} \cdot 3\text{H}_2\text{O}$ (Li,Al-LDH-CuY): Al, 14.26/13.74; Li, 1.75/1.77; Cu, 7.98/8.09; Cl, 0.49/0; C, 15.29/15.29; H, 4.58/4.62; N, 3.38/3.57. For $\text{Na}_2\text{NiC}_{10}\text{H}_{12}\text{N}_2\text{O}_8 \cdot 4\text{H}_2\text{O}$ (Na_2NiY): Na, 9.89/9.89; Ni, 12.61/12.62; C, 28.93/25.83; H, 4.74/4.33; N, 6.59/6.03. For $\text{Na}_2\text{CoC}_{10}\text{H}_{12}\text{N}_2\text{O}_8 \cdot 2\text{H}_2\text{O}$ (Na_2CoY): Na, 11.53/10.71; Co, 13.94/13.73; C, 26.35/27.99; H, 3.76/4.37; N, 5.97/6.53. For $\text{Na}_2\text{CuC}_{10}\text{H}_{12}\text{N}_2\text{O}_8 \cdot 3.5\text{H}_2\text{O}$ (Na_2CuY): Na, 10.58/9.98; Cu, 13.84/13.79; C, 25.91/26.07; H, 4.33/4.16; N, 5.82/6.08.

Synthesis of Li,Al-LDH-HY/MA₂. The intercalates Li,Al-LDH-HY/MA₂ were prepared by suspending 1 g of Li,Al-LDH-HY in 40 mL of 4.2×10^{-2} M aqueous solutions of the MA₂ salts {M = Co²⁺, Ni²⁺, and Cu²⁺; A = Cl⁻, NO₃⁻, and CH₃COO⁻ (Ac⁻)}. The reaction mixtures were kept at room temperature for 1 h with constant stirring. The final products were isolated by filtration, then washed with deionized water, and dried at ~50 °C in air.

Anal. Found/calcd (%). For $[\text{Li}_{0.66}\text{Al}_2(\text{OH})_6](\text{CoC}_{10}\text{H}_{12}\text{N}_2\text{O}_8)_{0.33} \cdot 2\text{H}_2\text{O}$ (Li,Al-LDH-HY/CoAc₂): Al, 17.80/17.34; Li, 1.54/1.49; Co, 6.21/6.25; C, 11.56/12.74; H, 4.58/4.52; N, 2.59/2.97. For $[\text{Li}_{0.66}\text{Al}_2(\text{OH})_6](\text{NiC}_{10}\text{H}_{12}\text{N}_2\text{O}_8)_{0.33} \cdot 2.5\text{H}_2\text{O}$ (LDH-HY/Ni(Ac)₂): Al, 17.12/16.86; Li, 1.44/1.44; Ni, 6.18/6.05; C, 11.40/12.38; H, 4.08/4.71; N, 2.43/2.89. For $[\text{Li}_{0.66}\text{Al}_2(\text{OH})_6](\text{CuC}_{10}\text{H}_{12}\text{N}_2\text{O}_8)_{0.33} \cdot 2\text{H}_2\text{O}$ (Li,Al-LDH-HY/Cu(Ac)₂): Al, 17.63/17.25; Li, 1.46/1.48; Cu, 7.18/6.71; C, 11.95/12.67; H, 3.98/4.50; N, 2.62/2.96. For $[\text{Li}_{0.75}\text{Al}_2(\text{OH})_6](\text{CoC}_{10}\text{H}_{12}\text{N}_2\text{O}_8)_{0.25} \cdot 2.5\text{H}_2\text{O}$ (LDH-HY/CoCl₂): Al, 18.00/17.87; Li, 1.72/1.72; Co, 4.34/4.88; Cl, 2.81/2.94; C, 10.29/9.95; H, 4.26/4.67; N, 2.17/2.32. For $[\text{Li}_{0.75}\text{Al}_2(\text{OH})_6](\text{NiC}_{10}\text{H}_{12}\text{N}_2\text{O}_8)_{0.25} \cdot 3\text{H}_2\text{O}$ (Li,Al-LDH-HY/NiCl₂): Al, 17.28/17.36; Li, 1.60/1.67; Ni, 4.05/4.72; Cl, 3.08/2.85; C, 9.79/9.66; H, 4.26/4.86; N, 2.04/2.25. For $[\text{Li}_{0.75}\text{Al}_2(\text{OH})_6](\text{CuC}_{10}\text{H}_{12}\text{N}_2\text{O}_8)_{0.25} \cdot 2.5\text{H}_2\text{O}$ (Li,Al-LDH-HY/CuCl₂): Al, 18.17/17.61; Li, 1.60/1.72; Cu, 5.78/5.24; Cl, 2.81/2.92; C, 10.86/9.91; H, 4.17/4.66; N, 2.26/2.31. For $[\text{Li}_{0.8}\text{Al}_2(\text{OH})_6](\text{CoC}_{10}\text{H}_{12}\text{N}_2\text{O}_8)_{0.25}(\text{NO}_3)_{0.2}(\text{H}_2\text{C}_{10}\text{H}_{13}\text{N}_2\text{O}_8)_{0.05} \cdot 2.5\text{H}_2\text{O}$ (Li,Al-LDH-HY/Co(NO₃)₂): Al, 17.23/16.85; Li, 1.97/1.73; Co, 4.06/4.60; C, 10.94/11.25; H, 4.38/4.63; N, 3.50/3.50. For $[\text{Li}_{0.8}\text{Al}_2(\text{OH})_6](\text{NiC}_{10}\text{H}_{12}\text{N}_2\text{O}_8)_{0.25}(\text{NO}_3)_{0.2}(\text{H}_2\text{C}_{10}\text{H}_{13}\text{N}_2\text{O}_8)_{0.05} \cdot 2.5\text{H}_2\text{O}$ (Li,Al-LDH-HY/Ni(NO₃)₂): Al, 16.76/16.85; Li, 1.78/1.73; Ni, 5.01/4.58; C, 10.76/11.25; H, 4.32/4.63; N, 3.17/3.50. For $[\text{Li}_{0.8}\text{Al}_2(\text{OH})_6](\text{CuC}_{10}\text{H}_{12}\text{N}_2\text{O}_8)_{0.25}(\text{NO}_3)_{0.2}(\text{H}_2\text{C}_{10}\text{H}_{13}\text{N}_2\text{O}_8)_{0.05} \cdot 3\text{H}_2\text{O}$ (Li,Al-LDH-HY/Cu(NO₃)₂): Al, 16.36/16.33; Li, 1.67/1.68; Cu, 5.59/4.81; C, 10.86/10.90; H, 4.19/4.79; N, 3.45/3.39.

The chemicals used in the syntheses were purchased from either Aldrich or Reachim, with purities above 98%.

Instrumentation. Powder X-ray diffraction (XRD) patterns were recorded with a Philips PW1710 diffractometer using Cu K α radiation with a scan speed 2° (2 θ)/min. IR spectra were recorded with a Perkin-Elmer 1600 FTIR spectrometer using KBr pellets. UV-vis diffuse reflectance spectra were recorded with a VSU-2P spectrometer using MgCO₃ as a standard.

Time-resolved in-situ energy-dispersive X-ray diffraction experiments (EDXRDs) were performed on Station 16.4 of the U.K. Synchrotron Radiation Source, Daresbury Laboratory, U.K., using an experimental setup which has been described elsewhere.²⁴ Individual spectra were collected with acquisition times of 30 s and a fixed detector angle (2 θ) of 1.80°, which provided a *d* spacing range ~5–20 Å. Analysis of the diffraction peaks was performed

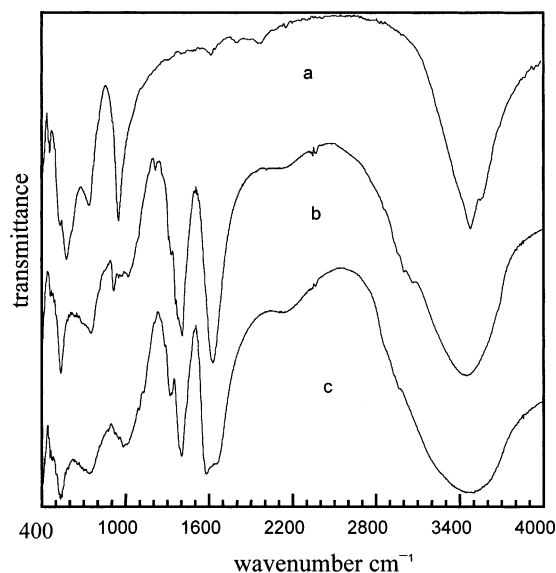


Figure 1. IR spectra of the intercalates: (a) Li,Al-LDH-Cl; (b) Li,Al-LDH-H₂Y; (c) Li,Al-LDH-HY.

by integrating the peak intensities using a Gaussian fitting routine. All the synthetic conditions in EDXRDs were repeated as in the laboratory, except the reaction vessel, which was replaced by a glass tube to fit the experimental cell.

Results and Discussion

Synthesis of Li,Al-LDH-HnY Intercalates. The treatment of Li,Al-LDH-Cl with solutions of Na₂H₂Y at pH = 4.5 and 8.0 leads to almost complete deintercalation of Cl⁻ and intercalation of H₂Y²⁻ and HY³⁻, respectively. Chemical analysis of mother liquors showed that the aluminum content did not exceed 2%, indicating that no significant dissolution of the Li,Al-LDH host had taken place. Elemental analysis of the solid products showed that their compositions correspond closely to the formula $[\text{LiAl}_2(\text{OH})_6](\text{H}_2\text{Y})_{0.5} \cdot 2.5\text{H}_2\text{O}$ and $[\text{LiAl}_2(\text{OH})_6](\text{HY})_{0.33} \cdot 2.5\text{H}_2\text{O}$, respectively. As seen from their IR spectra (Figure 1), the materials exhibit bands which are characteristic of the ligand: poorly resolved ν -CH vibrations at 2900–3000 cm⁻¹, ν -CN vibrations at ~1100 cm⁻¹, and strong asymmetrical and symmetrical ν -COO vibrations at ~1600 and ~1400 cm⁻¹, respectively. The IR spectra also display bands attributable to the Li,Al-LDH matrix: δ -AlOH (~960 cm⁻¹), ν -AlOH (~750 cm⁻¹), and δ -AlO₆ (~530 cm⁻¹) vibrations. Comparing the spectra of Li,Al-LDH-H₂Y and Li,Al-LDH-HY shows that the treatment at higher pH causes a significant decrease in absorbance of the band at 1615 cm⁻¹ and increase in absorbance of the band at 1580 cm⁻¹. We believe this is due to the decrease in the protonation of the intercalated ligand.

The powder XRD patterns indicate that intercalation of the EDTA ligand into Li,Al-LDH-Cl gives rise to a significant increase of interlayer separation from 7.65 to 12.1

(24) Clark, S. M.; Nield, A.; Rathbone, T.; Flaherty, J.; Tang, C. C.; Evans, J. S. O.; Francis, R. J.; O'Hare, D. *Nucl. Instrum. Methods* **1995**, *97*, 98. Clark, S. M.; Cernik, R. J.; Grant, A.; York, S.; Atkinson, P. A.; Gallagher, A.; Stokes, D. G.; Gregory, S. R.; Harris, N.; Smith, W.; Hancock, M.; Miller, M. C.; Ackroyd, K.; Farrow, R.; Francis, R. J.; O'Hare, D. *Mater. Sci. Forum* **1996**, *228*, 213.

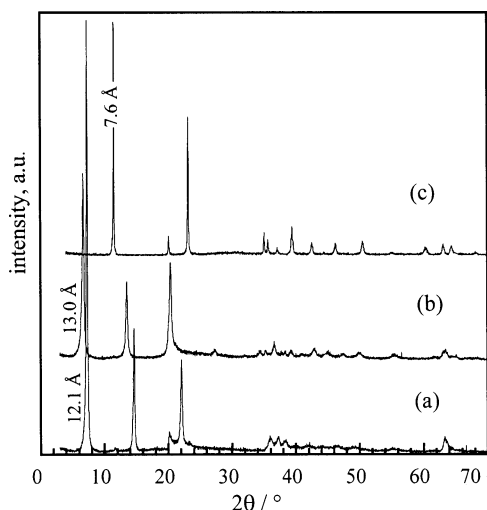


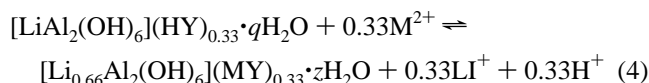
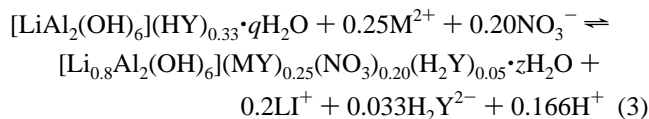
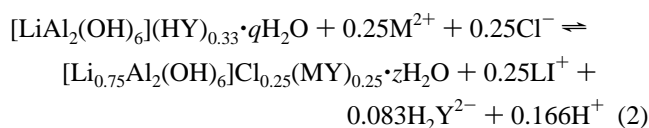
Figure 2. Powder XRD patterns of the intercalates: (a) Li,Al-LDH-HY; (b) Li,Al-LDH-H₂Y; (c) Li,Al-LDH-Cl.

Å (Li,Al-LDH-HY) and 13.0 Å (Li,Al-LDH-H₂Y) (Figure 2). The difference ~ 1 Å in d_{002} spacing (based on a hexagonal unit cell²⁰) of the products can be explained by different densities of the ligand in the LDH structure: a decrease of the anion concentration within the interlayer space allows the ligand to accommodate more spaciouly, causing a decrease in d spacing. Taking into account the dimensions of the EDTA ions,²⁵ one may conclude that the gallery size of the interlayer space derivable by subtraction of the thickness of the basal layer ~ 4.8 Å from d_{002} is not enough for the vertical accommodation of the ligand relative to the layers (Figure 3a). Otherwise, d_{002} would reach at least 16 Å. This is also confirmed by the fact that upon chelating metal cations an increase rather than a decrease in d_{002} spacing (as one could expect) is observed (see below). It is also worth noting that the d_{002} values found for Li,Al-LDH-HY and Li,Al-LDH-H₂Y are close to those found for Mg,Al-LDH-H_nnta⁽³⁻ⁿ⁾⁻ (11.8–13.3 Å)⁵ and Zn,Cr-LDH-nta³⁻ (12.1 Å).⁶ The coincidence may be not accidental, since both ligands contain the same R-N(CH₂COO⁻)₂ moiety, where R = CH₂COO⁻ (nta³⁻) or -CH₂CH₂N(CH₂COO⁻)₂ (edta⁴⁻), so it can be assumed that the character of the accommodation of EDTA and NTA may be similar. However, considering that the ligands have quite flexible skeletons, it would be unreasonable to choose their most probable orientations within interlayer space using only data obtained from powder XRD (Figure 3b).

Synthesis of Li,Al-LDH-HY/MA₂ Intercalates. The intercalates LDH-H_nY ($n = 1-2$) were treated with a solution of either cobalt, nickel, and copper nitrates, chlorides, or acetates. In the case of Li,Al-LDH-H₂Y, such treatment did not produce a simple ion-exchange intercalation reaction. On stirring Li,Al-LDH-H₂Y with a solution of the metal salts, a significant part of the LDH dissolved, forming a gellike mass. This is possibly due to the erosion of hydroxide layers by protons releasing from the ligand.

However, in the case of Li,Al-LDH-HY we did not observe any marked dissolution of the host, presumably as a result of a few released protons in this case. Therefore, all further experiments were performed using the Li,Al-LDH-HY material.

Addition of Li,Al-LDH-HY to aqueous solutions of the metal salts was accompanied with rapid (for several minutes) decoloration of the initial solutions and concomitant coloration of the solid phase. This suggests that the metal dications in each case have moved from solution into the solid phase—also confirmed by elemental analysis (Table 1). The kinetics of this process will be discussed below. As can be seen from the table, the compositions of the final products depend on the anions, rather than on the metals in the salts MA₂ taken for the treatment. In general terms the interactions of the metal salts with Li,Al-LDH-HY can be described by the following equations:



Therefore treatment of Li,Al-LDH-HY with the chloride and nitrate salts leads to the intercalation of the metal dications and the anions and partial de-intercalation of the ligand, lithium cations and protons (eqs 2 and 3). The intercalation of nitrate anions into the host is suggested by the elemental composition of the products and was later confirmed by IR spectroscopy. The reaction of Li,Al-LDH-HY with metal acetates proceeds by intercalation of cations without the counterions, and the introduction of the positive charge is compensated for entirely by the release from LDHs of the equivalent quantity of lithium and hydrogen cations. This difference in behavior may be due to the fact that acetate intercalates into LDH with more difficulty: in the series of selectivity in relation to anion exchange in Li,Al-LDH, it stands after chloride and nitrate: $\text{SO}_4^{2-} > \text{Cl}^- > \text{NO}_3^- \approx \text{CO}_3^{2-}/\text{HCO}_3^- > \text{CH}_3\text{COO}^-$.²⁶

XRD patterns show an increase of the interlayer separation from ~ 12 to ~ 15 Å (Figure 4). This could be caused by a change in conformation of the ligand within the interlayer space upon chelating the incoming metal cations. The estimated gallery height is 10 Å and is in close agreement with the maximal dimensions (9–10 Å) of some related complex salts K₂[CuY]·3H₂O, Ca[NiY]·4H₂O, and Ca[Co(H₂O)Y]·4H₂O as determined by single-crystal XRD experiments.²⁷ We conclude that metal complex ions in the LDH structure are accommodated without any apparent deforma-

(25) Julian, M. O.; Day, V. W.; Hoard, J. L. *Inorg. Chem.* **1973**, *12*, 1754. Cotrait, M. *Acta Crystallogr., Sect. B* **1970**, *26*, 1152. Cisarova, I.; Podlahova, J.; Podlaha, J. *Collect. Czech. Chem. Commun.* **1995**, *60*, 820.

(26) Mascolo, G. *Miner. Petrogr. Acta* **1985**, *29A*, 163.

(27) Porai-Koshits, M. A.; Polynova, T. N. *Koord. Khim.* **1984**, *10*, 725.

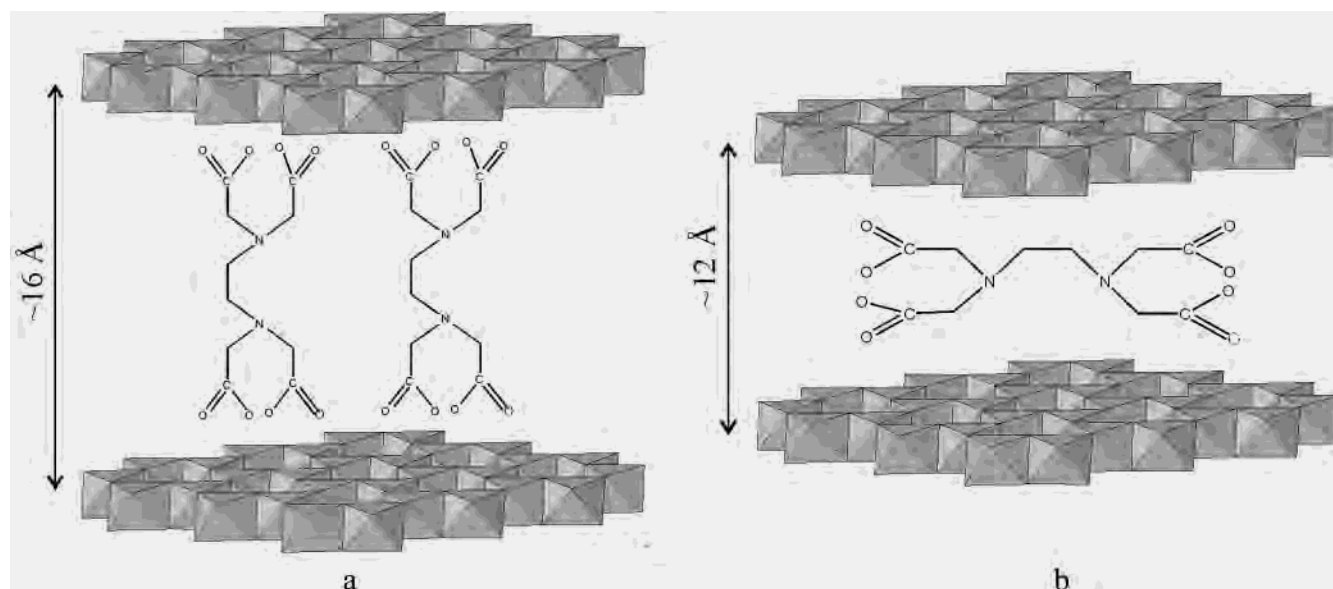


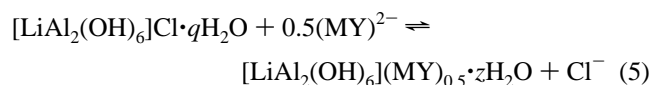
Figure 3. Schematic representations of two of the many potential orientations for the edta^{4-} ligand within an LDH.

Table 1. Summary of Elemental Analysis and Powder XRD for the Metal–edta Intercalates

material (idealized formula)	Li/Al	M/Li	M/Al	Cl/Al	C/N	d_{002} , Å
$[\text{LiAl}_2(\text{OH})_6]\text{Cl}\cdot 0.5\text{H}_2\text{O}$	0.514			0.521		7.65
$[\text{LiAl}_2(\text{OH})_6](\text{HY})_{0.33}\cdot 2.5\text{H}_2\text{O}$	0.471			0.004	5.10	12.1
$[\text{Li}_{0.66}\text{Al}_2(\text{OH})_6](\text{CoY})_{0.33}\cdot 2\text{H}_2\text{O}^a$	0.335	0.476	0.167		5.21	14.8
$[\text{Li}_{0.66}\text{Al}_2(\text{OH})_6](\text{NiY})_{0.33}\cdot 2.5\text{H}_2\text{O}^a$	0.326	0.509	0.166		5.48	14.7
$[\text{Li}_{0.66}\text{Al}_2(\text{OH})_6](\text{CuY})_{0.33}\cdot 2\text{H}_2\text{O}^a$	0.322	0.537	0.173		5.31	14.8
$[\text{Li}_{0.75}\text{Al}_2(\text{OH})_6]\{\text{Cl}_{0.25}(\text{CoY})_{0.25}\}\cdot 2.5\text{H}_2\text{O}^b$	0.371	0.300	0.111	0.119	5.53	14.8
$[\text{Li}_{0.75}\text{Al}_2(\text{OH})_6]\{\text{Cl}_{0.25}(\text{NiY})_{0.25}\}\cdot 3\text{H}_2\text{O}^b$	0.359	0.300	0.108	0.136	5.61	14.8
$[\text{Li}_{0.75}\text{Al}_2(\text{OH})_6]\{\text{Cl}_{0.25}(\text{CuY})_{0.25}\}\cdot 2.5\text{H}_2\text{O}^b$	0.341	0.395	0.135	0.118	5.62	14.7
$[\text{Li}_{0.8}\text{Al}_2(\text{OH})_6]\{(\text{CoY})_{0.25}(\text{NO}_3)_{0.2}(\text{H}_2\text{Y})_{0.05}\}\cdot 2.5\text{H}_2\text{O}^c$	0.443	0.245	0.109		3.65	14.8
$[\text{Li}_{0.8}\text{Al}_2(\text{OH})_6]\{(\text{NiY})_{0.25}(\text{NO}_3)_{0.2}(\text{H}_2\text{Y})_{0.05}\}\cdot 2.5\text{H}_2\text{O}^c$	0.412	0.333	0.137		3.97	14.7
$[\text{Li}_{0.8}\text{Al}_2(\text{OH})_6]\{(\text{CuY})_{0.25}(\text{NO}_3)_{0.2}(\text{H}_2\text{Y})_{0.05}\}\cdot 3\text{H}_2\text{O}^c$	0.396	0.366	0.145		3.68	14.8
$[\text{LiAl}_2(\text{OH})_6](\text{CoY})_{0.5}\cdot 3\text{H}_2\text{O}^d$	0.496	0.492	0.244	0.097	5.22	14.8
$[\text{LiAl}_2(\text{OH})_6](\text{NiY})_{0.5}\cdot 3\text{H}_2\text{O}^d$	0.438	0.496	0.217	0.025	5.24	14.8
$[\text{LiAl}_2(\text{OH})_6](\text{CuY})_{0.5}\cdot 3\text{H}_2\text{O}^d$	0.477	0.498	0.238	0.055	5.28	14.8

^a Formed by direct reaction of $[\text{LiAl}_2(\text{OH})_6]\text{HY}$ with $\text{M}(\text{Ac})_2$ salts (eq 4). ^b Formed by direct reaction described by eq 2. ^c Formed by direct reaction described by eq 3. ^d Formed by direct reaction as described by eq 5.

tions. For comparison we summarized in Figure 4 and Table 1 the XRD data for the intercalates formed by the direct ion-exchange reaction of Li,Al-LDH-Cl with $[\text{MY}]^{2-}$ ions according to eq 5.



The XRD patterns of the intercalates containing the $[\text{MY}]^{2-}$ complexes formed by different synthetic routes are in good agreement. The only difference is that the Bragg reflections in the XRD patterns of intercalates prepared by reaction of a preformed Li,Al-LDH-HY with the metal salts are broader and have lower intensity than the equivalent reflections for the samples prepared by direction anion exchange of the $[\text{MY}]^{2-}$ anions into Li,Al-LDH-Cl . The continued observation of Bragg reflections with $d \sim 4.4$ and 1.47 Å in $\text{Li,Al-LDH-HY/M}(\text{Ac})_2$, which can be indexed as ($h00$) by the analogy with the unit cell of Li,Al-LDH-Cl , indicates retention of the significant order in the ab -plane.

Equations 2–4 show that the treatment of Li,Al-LDH-HY with either chloride and nitrate salts, unlike acetate salts, makes the solid-state chelation within the LDH a complicated process, which involves intercalation and de-intercalation of several ionic species. As one can notice, atomic ratios M/Cl and M/NO_3 in the solids are close to 1. This implies that Cl^- and NO_3^- can insert into the interlayer space with M^{2+} as ion couples. Together with water molecules, these anions likely occupy positions among the ligands, and the partial de-intercalation of the ligand anions is caused by competition for vacant positions within the interlayer.

Interaction of Li,Al-LDH-HY with cobalt, nickel, and copper salts does not cause significant changes in positions and intensity of the IR bands, attributable to the hydroxide layers. Comparison of the spectra of salts $\text{Na}_2[\text{MY}]\cdot n\text{H}_2\text{O}$ and intercalates LDH-MY and $\text{LDH-HY/M}(\text{Ac})_2$ shows a good coincidence of the majority of the characteristic bands (Figure 5, Table 2). The most intense absorption bands are those belonging to carboxylates, at 1400 and 1600 cm^{-1} , that are a characteristic of coordinated COO groups. Following the transformation of Li,Al-LDH-HY into Li,Al-LDH-HY/

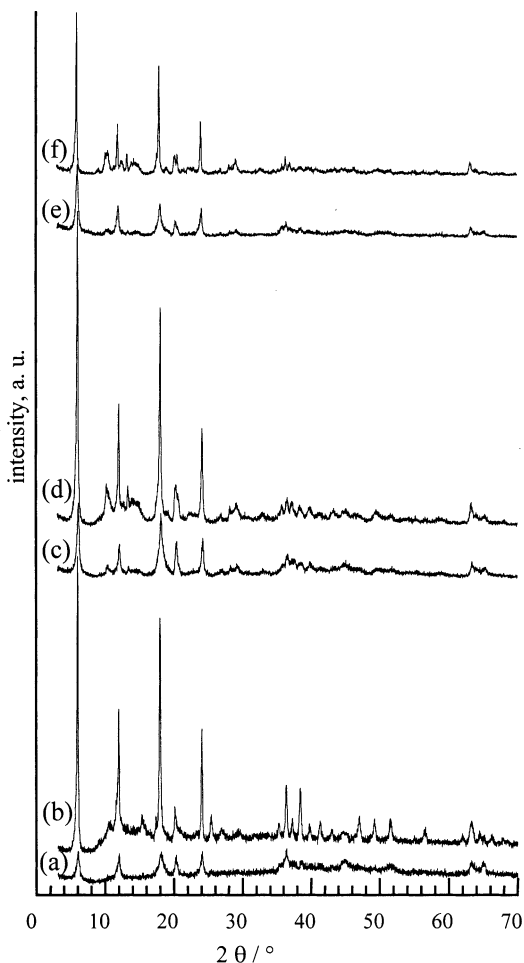


Figure 4. Powder XRD patterns of LDHs containing edta-chelated metal cations: (a) $[\text{Li}_{0.66}\text{Al}_2(\text{OH})_6](\text{CuY})_{0.33}\cdot 2\text{H}_2\text{O}$; (b) $[\text{LiAl}_2(\text{OH})_6](\text{CuY})_{0.5}\cdot 3\text{H}_2\text{O}$; (c) $[\text{Li}_{0.66}\text{Al}_2(\text{OH})_6](\text{NiY})_{0.33}\cdot 2.5\text{H}_2\text{O}$; (d) $[\text{LiAl}_2(\text{OH})_6](\text{NiY})_{0.5}\cdot 3\text{H}_2\text{O}$; (e) $[\text{Li}_{0.66}\text{Al}_2(\text{OH})_6](\text{CoY})_{0.33}\cdot 2\text{H}_2\text{O}$; (f) $[\text{LiAl}_2(\text{OH})_6](\text{CoY})_{0.5}\cdot 3\text{H}_2\text{O}$.

$\text{M}(\text{Ac})_2$ the shape of the band of the asymmetrical COO vibrations notably changes: the maximum at 1580 cm^{-1} and the shoulder at 1660 cm^{-1} merge into one absorption with a maximum at $1600\text{--}1610\text{ cm}^{-1}$. This provides some evidence for the coordination of the carboxylates to the transition metal ions. Some authors have interpreted the merging of this absorption as proof of the equivalence of the COO⁻ groups of the ligand after chelating metals.¹⁵ IR spectroscopy has been used to try and provide information of the nature of the metal–ligand interactions in metal–EDTA complexes. Logvinenko et al. have investigated the IR spectra of the complexes $\text{M}_1\text{M}_2\text{Y}\cdot\text{H}_2\text{O}$ ($\text{M}_1 = \text{Mg}, \text{Ca}$; $\text{M}_2 = \text{Co}^{2+}, \text{Ni}^{2+}, \text{Mn}^{2+}, \text{Cu}^{2+}$; $\text{Y} = \text{edta}^{4-}$).²⁹ The structures of these complexes have already been determined by single-crystal XRD analysis. In fact $\text{MgNiY}\cdot 6\text{H}_2\text{O}$ (hexadentate EDTA) had a split absorption band at 1600 cm^{-1} , while $\text{CaCoY}\cdot 5\text{H}_2\text{O}$ (pentadentate EDTA) exhibits an unsplit COO absorption. As the authors report, this behavior can be explained by the high sensitivity of the asymmetrical vibrations of coordinated COO⁻ groups to intermolecular interactions, especially hydrogen bonding.

(29) Logvinenko, V. A.; Myachina, L. I.; Ipatova, T. B. *Izv. Sib. Otd. Ross. Akad. Nauk, Sib. Khim. Zh.* **1980**, *12*, 41.

(30) Jørgensen, C. K. *Acta Chem. Scand.* **1955**, *3*, 1362.

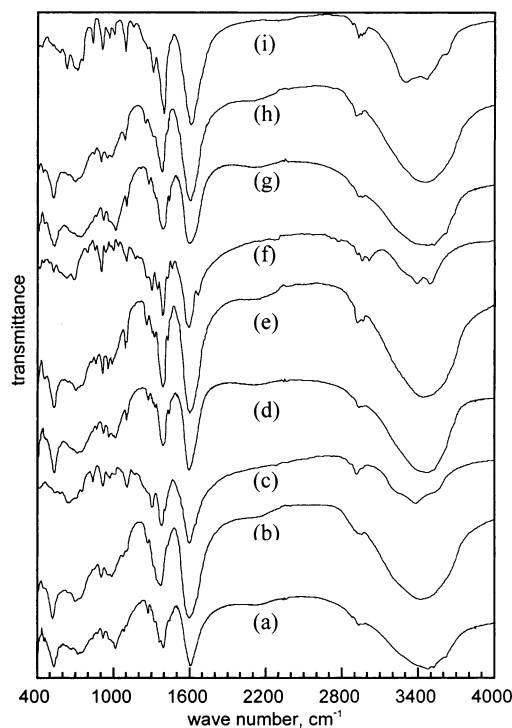


Figure 5. IR spectra of the metal edta salts and the LDHs containing edta-chelated metal cations: (a) $[\text{Li}_{0.66}\text{Al}_2(\text{OH})_6](\text{CuY})_{0.33}\cdot 2\text{H}_2\text{O}$; (b) $[\text{LiAl}_2(\text{OH})_6](\text{CuY})_{0.5}\cdot 3\text{H}_2\text{O}$; (c) $\text{Na}_2\text{CuY}\cdot 3.5\text{H}_2\text{O}$; (d) $[\text{Li}_{0.66}\text{Al}_2(\text{OH})_6](\text{NiY})_{0.33}\cdot 2.5\text{H}_2\text{O}$; (e) $[\text{LiAl}_2(\text{OH})_6](\text{NiY})_{0.5}\cdot 3\text{H}_2\text{O}$; (f) $\text{Na}_2\text{NiY}\cdot 4\text{H}_2\text{O}$; (g) $[\text{Li}_{0.66}\text{Al}_2(\text{OH})_6](\text{CoY})_{0.33}\cdot 2\text{H}_2\text{O}$; (h) $[\text{LiAl}_2(\text{OH})_6](\text{CoY})_{0.5}\cdot 3\text{H}_2\text{O}$; (i) $\text{Na}_2\text{CoY}\cdot 2\text{H}_2\text{O}$.

The UV–vis spectra for Li,Al-LDH–MY, Li,Al-LDH–HY/ $\text{M}(\text{Ac})_2$ and $\text{Na}_2\text{MY}\cdot x\text{H}_2\text{O}$ ($\text{M} = \text{Co}, \text{Ni},$ and Cu) have been recorded and are shown in Figure 6. Values for absorption maxima are presented in Table 3, in addition to literature data of the $[\text{MY}]^{2-}$ complexes in aqueous solution. We observe that in all cases, except the ${}^4\text{T}_{1g} \rightarrow {}^4\text{T}_{2g}$ transition of $[\text{CoY}]^{2-}$, there is a blue shift of the metal-based d–d bands for Li,Al-LDH–HY/ MA_2 and Li,Al-LDH–MY in relation to those observed for $\text{Na}_2\text{MY}\cdot x\text{H}_2\text{O}$. The transition ${}^3\text{A}_{2g} \rightarrow {}^1\text{E}_{1g}$ observed as a shoulder at $810\text{--}820\text{ nm}$ ($\sim 12\,270\text{ cm}^{-1}$) in $\text{Na}_2\text{NiY}\cdot 4\text{H}_2\text{O}$ and Li,Al-LDH–HY/ $\text{Ni}(\text{Ac})_2$ is not seen in Li,Al-LDH–NiY. It is likely that in the spectra of LDH–NiY it is obscured by the intense transition ${}^3\text{A}_{2g} \rightarrow {}^3\text{T}_{2g}$. Although this transition is spin-forbidden, it is known to be a characteristic for Ni^{2+} in the high-spin state. Taking all the analytical, structural, and spectroscopic data into consideration, we propose a schematic representation of the Li,Al-LDH–HY/ MA_2 phases in Figure 7.

Kinetic Experiments. The kinetics of the solid-state chelation of the metal cations by EDTA intercalated in Li,Al-LDH phases has been studied using time-resolved, in-situ energy-dispersive X-ray powder diffraction (EDXRD). The EDXRD data revealed that the reaction of Li,Al-LDH–HY with either $\text{Ni}(\text{NO}_3)_2$, NiCl_2 , $\text{Co}(\text{Ac})_2$, or $\text{Cu}(\text{Ac})_2$ was too rapid to be amenable to study by this technique, since the first EDXRD dataset following mixing of the reagents showed only the Bragg reflections of the final crystalline products. Fortunately, the reaction of Li,Al-LDH–HY with nickel acetate is sufficiently slow to be able to follow using the diffraction techniques. There seems to be no correlation

Table 2. Summary of Selected IR Data and Assignments for the Metal–edta Intercalates^a

material	assignment				
	ν -CH	ν -COO _{asym}	ν -COO _{sym}	ν -CN	δ -AlOH
[LiAl ₂ (OH) ₆]Cl·0.5H ₂ O Na ₂ CuY·1.5H ₂ O ²⁸	2930	1620 (δ -H ₂ O) 1605 (s)	1390 (s)	1130 1120	960
[Li _{0.66} Al ₂ (OH) ₆](CuY) _{0.33} ·2H ₂ O ^b	2972 2936 2883	1610 (s)	1397 (s)	1109 1087	970 920
[LiAl ₂ (OH) ₆](CuY) _{0.5} ·3H ₂ O ^c	2979 2937 2883	1605 (s)	1387 (s) 2937 2883	1156 (sh) 1104 (sh) 1080	959
Na ₂ CuY·1.5H ₂ O ²⁸	2950	1600 (s)	1395 (s)	1125 1110	
[Li _{0.66} Al ₂ (OH) ₆](CoY) _{0.33} ·2H ₂ O ^b	2936 2964 2886 (sh)	1604 (s)	1391 (s)	1106	964
[LiAl ₂ (OH) ₆](CoY) _{0.5} ·3H ₂ O ^c	2960 2928 2885 (sh)	1605 (s)	1391 (s)	1103	960 2928 2885 (sh)
Na ₂ NiY·4H ₂ O ²⁸	2950	1605	1400 (s) 1390 (sh)	1105	
[Li _{0.66} Al ₂ (OH) ₆](NiY) _{0.33} ·2.5H ₂ O ^b	2974 2960 2938 2886 (sh)	1604 (s)	1391 (s)	1106	964
[LiAl ₂ (OH) ₆](NiY) _{0.5} ·3H ₂ O ^c	2970 2931 2880 (sh)	1605 (s)	1391 (s) 2931 2880 (sh)	1112 1100	963

^a (s) = strong, (sh) = shoulder. ^b Formed by direct reaction of [LiAl₂(OH)₆]HY with M(Ac)₂ salts (eq 4). ^c Formed by direct reaction as described by eq 5.

Table 3. Summary of the UV–Vis Spectroscopy Data for the Metal–edta Intercalates^a

material	wavelength for given d–d transition, nm			
	⁴ T _{1g} → ⁴ T _{2g}	⁴ T _{1g} → ⁴ A _{2g}	⁴ T _{1g} → ⁴ T _{1g} (multiplet)	
CoY ²⁻ (aq) ³⁰	1100	613 (sh)	503, 485, 465	
Na ₂ CoY·2H ₂ O	950 (sh)	620	530, 480	
[LiAl ₂ (OH) ₆](CoY) _{0.5} ·3H ₂ O ^b	950	600	490 (sh), 460	
[Li _{0.66} Al ₂ (OH) ₆](CoY) _{0.33} ·2H ₂ O	1050 (sh)	595 (sh)	500, 460	
material	wavelength for given d–d transition, nm			
	³ A _{2g} → ³ T _{2g}	³ A _{2g} → ¹ E _{1g}	³ A _{2g} → ³ T _{1g} (F)	³ A _{2g} → ³ T _{1g} (P)
NiY ₂ (aq) ³⁰	990	790	587	382
Na ₂ NiY·4H ₂ O	1100	820 (sh)	600	400
[LiAl ₂ (OH) ₆](NiY) _{0.5} ·3H ₂ O ^b	880		580	380
[Li _{0.66} Al ₂ (OH) ₆](NiY) _{0.33} ·2.5H ₂ O ^c	975	810 (sh)	580	380
material	wavelength for given d–d transition, nm	material	wavelength for given d–d transition, nm	
	² E _g → ² T _{2g}		² E _g → ² T _{2g}	
CuY ₂ (aq) ³⁰	730	[LiAl ₂ (OH) ₆](CuY) _{0.5} ·3H ₂ O ^b	740	
Na ₂ CuY·3.5H ₂ O	760	[Li _{0.66} Al ₂ (OH) ₆](CuY) _{0.33} ·2H ₂ O ^c	740	

^a (sh) = shoulder. ^b Formed by direct reaction as described by eq 5. ^c Formed by direct reaction of [LiAl₂(OH)₆]HY with M(Ac)₂ salts (eq 4).

between the stability constants of the [MY]²⁻ complex formation and the rate of the solid-state chelation since log *K*(CoY) is more than 2 orders of magnitude less than log *K*(NiY). It is difficult to explain why the rate of intercalation of nickel ions in Li,Al-LDH–HY using Ni(Ac)₂ is slower than when using other nickel(II) salts.

The solid-state chelation/intercalation of nickel ions in Li,Al-LDH–HY using Ni(Ac)₂ was studied at three different Ni²⁺ ion concentrations: 0.027, 0.04, and 0.053 M. The two latter concentrations were taken to provide, respectively, an 1.5- and 2-fold excess of Ni²⁺ ions in relation to the chelation capacity of Li,Al-LDH–HY, whereas the former one was taken to provide the ratio HY:Ni = 1:1 (see eq 4).

Quantitative kinetic data were extracted by determining the integrated intensities of the Bragg reflections of the host and product phases. Unfortunately, the analysis was hindered by significant overlap of the Bragg reflections of the host and product. We were able to monitor the decay of the intensity of the 002 Bragg reflection of the starting material and have used these data in our subsequent kinetic analysis. The integrated peak of the 002 reflection were converted to the extent of the reaction, α , using the relationship

$$1 - \alpha_{hkl}(t) = I_{hkl}(t)/I_{hkl}(t_0) \quad (6)$$

Figure 8 shows the decay of the integrated intensity of the 002 Bragg reflection of Li,Al-LDH–HY at three different

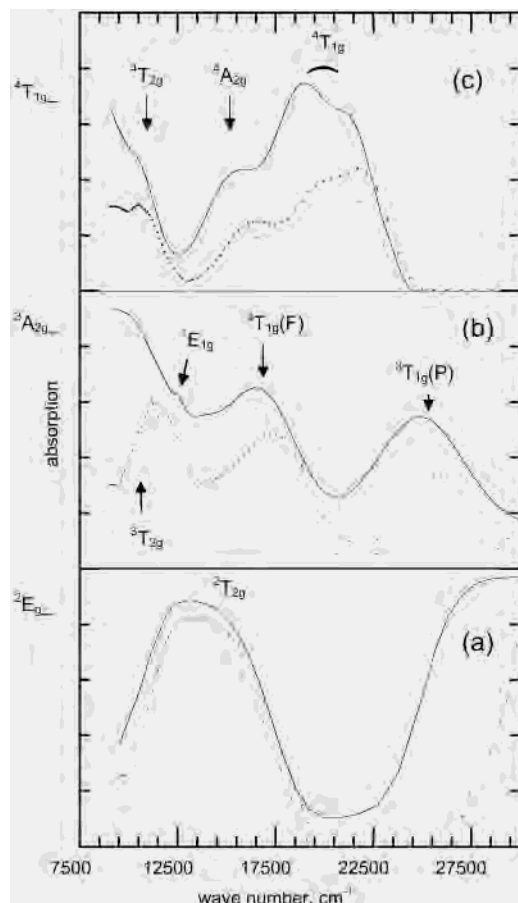


Figure 6. UV-vis diffuse reflectance spectra of the metal edta salts and the LDHs containing edta-chelated metal cations: (—) $\text{Na}_2\text{MY}\cdot x\text{H}_2\text{O}$; (---) $[\text{LiAl}_2(\text{OH})_6](\text{MY})_{0.5}\cdot z\text{H}_2\text{O}$; (· · ·) $[\text{Li}_{0.66}\text{Al}_2(\text{OH})_6](\text{MY})_{0.33}\cdot z\text{H}_2\text{O}$, $\text{M} =$ (a) Cu^{2+} , (b) Ni^{2+} , and (c) Co^{2+} .

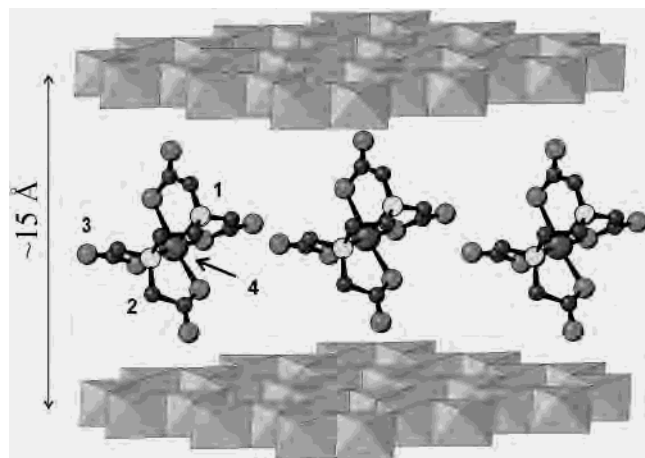


Figure 7. Schematic representation of the possible structure of a metal-edta chelate ($[\text{MY}]^{2-}$) intercalated in the interlayer space of an LDH. Water molecules are not depicted. Atom labeling: nitrogen (1), carbon (2), oxygen (3), and transition metal (4). Hydrogen atoms are omitted for clarity.

initial $\text{Ni}(\text{Ac})_2$ concentrations. The data were fitted to the Avrami-Erofe'ev rate expression, a kinetic model widely used in solid-state chemistry, and which has been used previously in intercalation studies.^{21,31}

$$\alpha = 1 - \exp[-(k(t-t_0))^m] \quad (7)$$

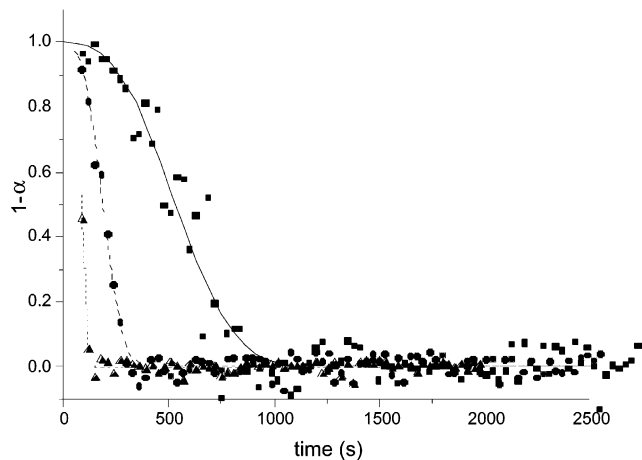


Figure 8. Time-resolved in-situ EDXRD data for the intercalation of Ni^{2+} ions in Li,Al-LDH-HY at 20°C . Plot shows the normalized integrated intensity of the 002 Bragg reflection of Li,Al-LDH-HY host after the addition of a $\text{Ni}(\text{Ac})_2$ solution at three different Ni^{2+} concentrations: (■) 0.027, (●) 0.04, and (▲) 0.053 M.

Table 4. Summary of the Kinetic Parameters^a

$[\text{NiAc}_2]$, mol/L	$t_{0.5}$, s	m	$k(m_0=3)$, s^{-3}	reacn order
0.027	535	2.9	1.57×10^{-3}	2.7
0.040	186	3.0	4.58×10^{-3}	

^a $t_{0.5}$ = time required to react at $\alpha = 0.5$. Kinetic parameters (k , m) obtained by least-squares fitting to eq 7.

The data show that the chelation/intercalation of Ni^{2+} cations in Li,Al-LDH-HY at an initial $\text{Ni}(\text{Ac})_2$ concentration of 0.053 M proceeds too quickly to be accurately measured using our diffraction method. Taking the two other Ni^{2+} ion concentrations, we were able to measure decay curves for the host material. The kinetic parameters extracted from these data are summarized in Table 4. Using formalism of Avrami-Erofe'ev kinetics, we can interpret the parameter $m = 3$ obtained in our experiment as an argument that the solid-state chelation can be a phase boundary controlled process. Although we have only two reliable data points, we estimate the order of the reaction with respect to $\text{Ni}(\text{Ac})_2$ concentration to be ~ 3 .

Conclusions

We have found that treatment of an Li,Al-LDH which has been pre-intercalated with EDTA ligands is able to chelate transition metal ions from aqueous solutions to form intercalated $[\text{M}(\text{edta})]^{2-}$ complexes. The ion-exchange capacity is calculated to be approximately 1.1 mmol/g. The details of the reaction depend on the nature of the anion associated with the transition metal cations in solution. Treatment of the LDH with solutions of either the metal chloride or nitrate salts leads to co-intercalation of either the Cl^- or NO_3^- anions, respectively. In the case of the metal acetate salts the cations intercalate without the accompanying anion. This can be explained by the different intercalation

(31) Price, S. J.; Evans, J. S. O.; Wong, H. V.; O'Hare, D. *J. Adv. Mater.* 1996, 8, 582.

Chelation of Metal Ions in a Double Hydroxide

selectivity of the anions in relation to the LDH. Kinetics experiments have revealed that these ion-exchange chelation/intercalations proceed for very short times. In the case of nickel acetate, the rate of the chelation/intercalation of Ni^{2+} ions was found to have a third-order dependence on the nickel acetate concentration $\{k \propto [\text{Ni}(\text{Ac})_2]^3\}$. Solid-state chelating agents that are able to immobilize metal ions in solid matrixes may potentially be of interest for recovering

toxic, environmentally unfriendly, and/or radioactive cations from aqueous solutions.

Acknowledgment. The authors thank the EPSRC for financial support and access to the SRS, Daresbury Laboratory, and the Royal Society and NATO for a fellowship to K.A.T.

IC0203926